InMotion hybrid racecar : F1 performance with LeMans endurance

Received 4 November 2013
Revised 4 February 2014
Accepted 19 October 2014

InMotion hybrid racecar: F1 performance with LeMans endurance

J. Jacob
TNO – Powertrains Research Group, Helmond, The Netherlands
J.A. Colin, H. Montemayor, D. Sepac, H.D. Trinh, S.F. Voorderhake and P. Zidkova
PDEng Automotive Systems Design, Stan Ackermans Institute, Eindhoven University of Technology, Eindhoven, The Netherlands, and
J.J.H. Paulides, A. Borisaljevic and E.A. Lomonova
Electromechanics and Power Electronics Group, Department of Electrical Engineering, Eindhoven University of Technology, Eindhoven, The Netherlands

Abstract

Purpose – The purpose of this paper is to demonstrate that using advanced powertrain technologies can help outperform the state of the art in F1 and LeMans motor racing. By a careful choice and sizing of powertrain components coupled with an optimal energy management strategy, the conflicting requirements of high-performance and high-energy savings can be achieved.

Design/methodology/approach – Five main steps were performed. First, definition of requirements: basic performance requirements were defined based on research on the capabilities of Formula 1 race cars. Second, drive cycle generation: a drive cycle was created using these performance requirements as well as other necessary inputs such as the track layout of Circuit de la Sarthe, the drag coefficient, the tire specifications, and the mass of the vehicle. Third, selection of technology: the drive cycle was used to model the power requirements from the powertrain components of the series-hybrid topology. Fourth, lap time sensitivity analysis: the impact of certain design decisions on lap time was determined by the lap time sensitivity analysis. Fifth, modeling and optimization: the design involved building the optimal energy management strategy and comparing the performance of different powertrain component sizings.

Findings – Five different powertrain configurations were presented, and several tradeoffs between lap time and different parameters were discussed. The results showed that the fastest achievable lap time using the proposed configurations was 3 min 9 s. It was concluded that several car and component parameters have to be improved to decrease this lap time to the required 2 min 45 s, which is required to outperform F1 on LeMans.

Originality/value – This research shows the capabilities of advanced hybrid powertrain components and energy management strategies in motorsports, both in terms of performance and energy savings. The important factors affecting the performance of such a hybrid race car have been highlighted.

Keywords Energy management strategy, Powertrain design, Race car dynamics, Series hybrid electric race car

Paper type Research paper

I. Introduction

Race cars are an excellent showcase for new technologies from the different areas of automotive systems. The InMotion project group utilizes the state-of-the-art research in the automotive domain that is being carried out at the Eindhoven University of Technology for the design of a high-tech and innovative race car. The aim for this race car will be able to drive autonomously around the race track Circuit de la Sarthe in

COMPEL: The International Journal for Computation and Mathematics in Electrical and Electronic Engineering
Vol. 34 No. 1, 2015
pp. 210-233

0332-1649
DOI 10.1108/COMPEL-11-2013-0344

France, with a lap time faster than a Formula 1 car. The designed vehicle will be a hybrid electric vehicle with the implementation of many advanced innovations.

Nowadays, hybrid powertrains have indeed become a topic of interest for racing vehicles. Formula 1 (2012 season) incorporates a Kinetic Energy Recovery System (KERS), which can store up to 400 kJ with a maximum power of 60 kW. One objective of introducing the KERS system is to promote the development of environmentally friendly and road car relevant technologies in Formula 1 racing (Formula 1,). Audi incorporates a flywheel accumulator system in the R-18 e-tron Quattro racing vehicle for the 24 hours of Le Mans race. This system can recover up to 500 kJ of energy while braking (Audi,). Lambert *et al.* (2008) proposed a methodology for the development of a hybrid electric racing car with the aim of increasing the maximum acceleration. It was found that different parallel architectures can increase acceleration performance with the use of an electric machine and energy storage system. Sibley and Emadi (2010) introduced a control analysis for hybrid electric vehicles designed for high-performance applications. It was concluded that the trade-off between efficiency and performance can be addressed by adding constraints on the driver's demand for quick acceleration and by using neural networks for optimization of the energy flow in the powertrain. Benson *et al.* (2005) explored the potential of a series hybrid gas electric propulsion system for a race vehicle designed for Formula SAE. The hybrid configuration includes ultracapacitors, a 206 cm^3 engine, a permanent magnet brushed generator, an induction motor, and a fixed-ratio gearbox. It was concluded that the hybrid powertrain can offer significant advantages in terms of acceleration. High-torque densities are a key requirement in traction machines. Using a multiple air gap design, as proposed in Paulides *et al.* (2011), up to 60 percent higher torque density relative to single air gap machines can be achieved (Figure 1).

At the start of the InMotion race car design project, the authors of this paper temporarily became part of the project team, and their task was to design a powertrain system. InMotion had the following goals with respect to the powertrain:

- The vehicle should have a high efficiency, which should be achieved by designing a hybrid electric powertrain that is controlled by an optimized energy management strategy.
- The hybrid powertrain should have a series hybrid topology. This is due to relative mechanical simplicity of the topology, when compared to other hybrid topologies.
- The performance in terms of cornering speed and acceleration should exceed that of a Formula 1 race car.
- The vehicle should have a higher durability than a Formula 1 car, i.e. be able to complete the 24 hours of Le Mans race.

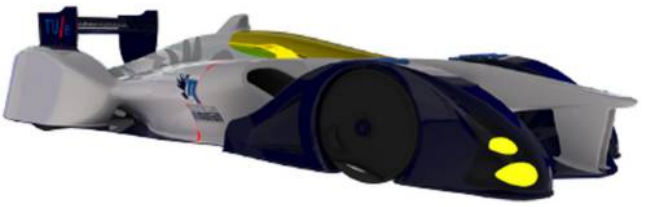

Figure 1.
Iso view of InMotion IM01

Background research was done on hybrid vehicle topologies and technologies. Based on the goals of InMotion, the steps to be taken in designing the powertrain were defined.

A. Background

Hybrid electric vehicles make use of the best characteristics of engine, motor, energy storage, and other complementary components. There are two main types of powertrain topologies: series and parallel. The series topology has the advantages of a simpler control strategy, mechanical simplicity, and the possibility to use a lightweight high-speed engine. The disadvantages include that when energy is being provided from the engine, the energy has to pass through both generator and motor, which increases the losses compared to the parallel topology. Moreover, in case there is no energy storage device, the motor, engine, and generators each have to be fully sized to meet the required power demand. This results in a relatively heavy powertrain, when compared to a conventional one. For the parallel topology, the engine size can be reduced because the engine can drive the wheels directly in combination with the electric motors. Furthermore, it is possible to use three driving modes which are engine only, motor only, or a combination of engine and motor. However, directly connecting the engine with the wheels requires a low-speed engine or large gear ratios. Together with the more complex transmission to be able to switch between the modes of operation, this makes for larger mechanical losses and a more complex control strategy. In both mentioned architectures, energy storage plays a very important role. Among the most known devices are battery, ultracapacitor, flywheel, fuel cell, and hydrogen supply.

The racing circuit consists mainly of sections where brisk acceleration and heavy braking are needed. On one hand, this implies a large power demand from the powertrain. On the other hand, this means that there is a possibility to regenerate an enormous amount of energy by regenerative braking. Modern batteries, especially those with Li-ion phosphate technology, are high in energy content. However, they are limited in terms of power and frequency of charging and discharging. In contrast, ultracapacitors have very high charging and discharging rates, but they are low in energy content.

Given this background on hybrid electric vehicles, a sequence of design steps had to be defined, which would help in designing a hybrid electric powertrain with the right technology choices and component sizings that would meet InMotion's requirements.

Five main steps were followed in the design process. First, the performance requirements were defined. Second, the drive cycle was generated using these performance requirements. Third, the most feasible technologies were selected for the powertrain components, based on which a preliminary electrical analysis of the powertrain was performed. Fourth, a laptime sensitivity analysis was performed to analyze the impact of certain design parameters on the lap time. Finally, the racecar's performance was modeled.

II. Definition of requirements

In this step of the design, performance requirements were defined based on the goals of InMotion. These requirements were derived based on research into Formula 1 race cars. In addition to these requirements, some design constraints were imposed so as to limit the design space.

A. Performance requirements

The goal of InMotion is to show that Formula 1 technology, although very advanced, does not represent state-of-the-art research due to rule restrictions. It is therefore very

important to beat a Formula 1 race car in every way possible. For this reason it was decided that the InMotion race car should accelerate faster than a Formula 1 race car, have a higher top speed, and hence have a shorter lap time on the Le Mans circuit. The required lap time was defined to be 2 min 45 s. This is a 10 s improvement on the estimated Formula 1 lap time on the Circuit de la Sarthe of 2 min 55 s (F1 Fanatic,). For the top speed, a speed of 350 km/h is used and the acceleration profile of the 2004 F1 was considered, since more recent data was not available. This acceleration profile is shown in Table I.

B. Design constraints

InMotion imposed certain constraints on the powertrain design, which were as follows:

- maximum weight for the energy storage is 250 kg for a single energy storage type and 350 kg for two storage types;
- the energy storage volume is limited to two times 0.072 m^3 with a base of 0.36 m^2;
- the DC-link voltage is limited to 1 kV; and
- no plug-in capability.

III. Drive cycle generation

Initially, the drive cycle was calculated to describe the velocity of the race car at each location on the track. To generate this drive cycle, the track layout was extracted as described in Section III-A. The tire friction coefficients, which represent an important limitation of the maximum speed achievable in the drivecycle, were estimated as shown in Section III-B. After that the velocity at each point was be determined. This velocity is calculated in three steps. First, the maximum velocity due to the limitation on the lateral force that can be generated by the tires, was calculated (i.e. the velocity at which the lateral force equals to the maximum that the tires can handle, this is described in Section III-C). Second, the limited braking power of the race car was taken into account (Section III-D). Finally, the acceleration performance was used (Section III-E).

The model used for the drive cycle was based on a bicycle model. Although the bicycle model has the disadvantage that it does not compute the lateral load transfers (body roll is not considered), its calculation time is very short compared to a full vehicle model. Besides, there were not enough data on vehicle parameters to build a full vehicle model. The speed was calculated first as a function of position, and then it was expressed as a function of time. In this way, it was possible to compare the calculated drive cycle to the drive cycle from the Audi R18 e-tron quattro race car (YouTube,).

A. Track layout

As mentioned in Section I, the track to be driven is the Circuit de la Sarthe, which is shown in Figure 2. Using Google Earth (Google,) and 3D Route Builder (Hybrid GeoTools,) from Hybrid GeoTools, the raceline across the circuit was identified and a GPS map including the altitude at each point was extracted. This GPS map was then

Table I. 2004 F1 acceleration profile as given by InMotion

Speed (km/h)	0	25	100	200	250	300	350
Time (s)	0	0.42	1.70	3.80	5.50	8.60	13.6

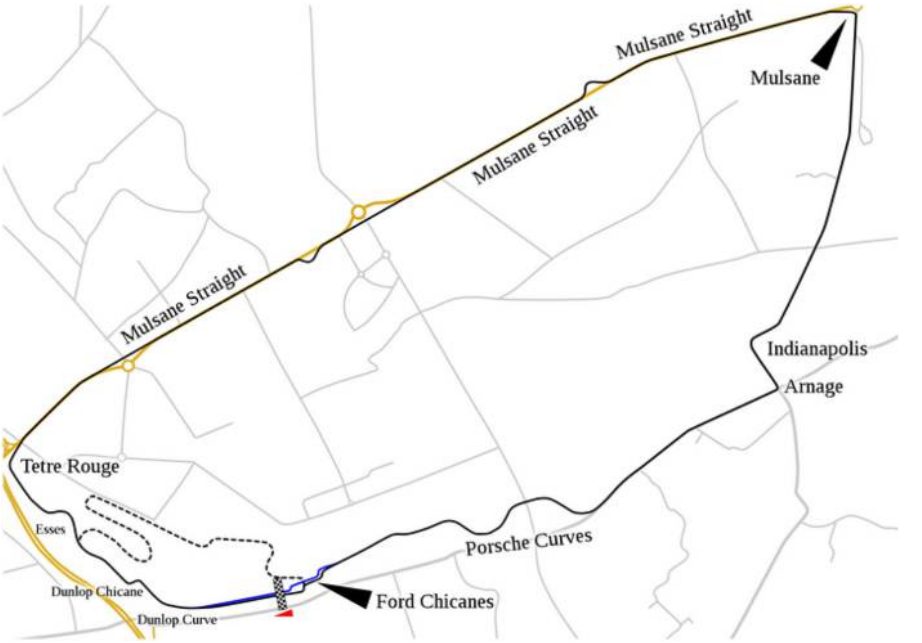

Figure 2.
Circuit de la Sarthe

Source: Le Mans, France

converted to a list of radii by calculating the circumradius of every three points as shown in Figure 3 using (Wolfram Mathworld,):

$$K = \sqrt{s(s-a)(s-b)(s-c)}, \tag{1}$$

where a, b, and c are the lengths (in m) of the sides of the triangle made of the three points and:

$$s = \frac{1}{2}(a+b+c) \tag{2}$$

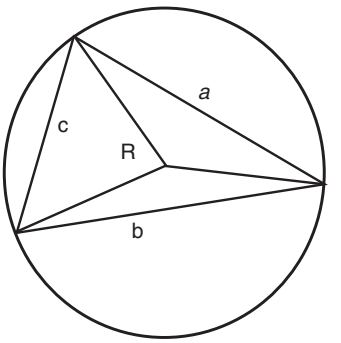

Figure 3.
Circumradius R of three points constituting a triangle having lengths of a, b, and c

Finally, the radius R (in m) is calculated with:

$$R = \frac{abc}{4K} \tag{3}$$

The radius calculated is said to be the radius of the middle point (i.e. point between sides a and b). The left hand corners were defined to be positive and right hand to be negative. The track layout, with all its parameters is shown in Figure 4. Once the track layout was defined, the next step was to identify the tire friction coefficients, which determine the maximum speed achievable in the drivecycle.

B. Tire friction coefficients

Other necessary inputs are the longitudinal and lateral friction coefficients of the tires. Dunlop Formula 3 tire data were chosen for design; on which a linear and quadratic fits were created as shown in Figure 5. The difference between the linear and quadratic fit was negligible up to a normal force of 4,000 N (0.002 and 0.025 for the longitudinal and lateral friction coefficient, respectively). Therefeore, the linear

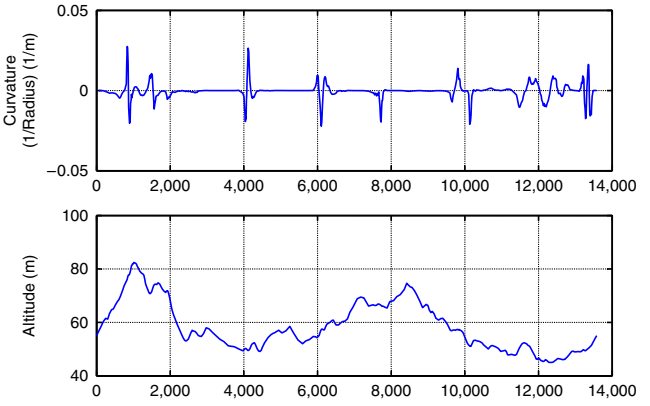

Figure 4.
Top: inverse radius to clearly identify the corners; bottom: drag coefficient

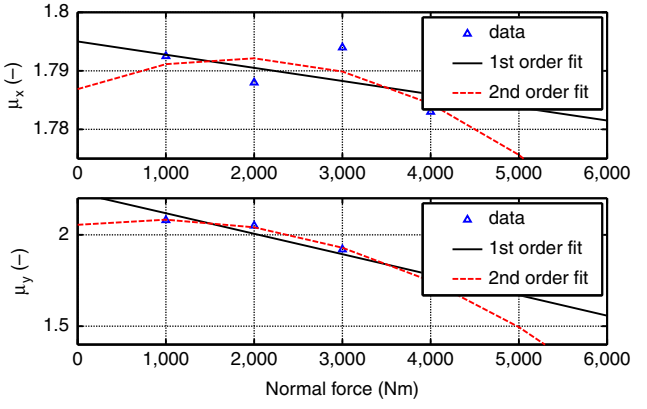

Figure 5.
First- and second- order fit on Dunlop Formula 3 tire data

fit was chosen because of its simplicity. The friction coefficients in lateral and longitudinal directions are:

$$\mu_x = 2.21 + (-1.05) \cdot 10^{-4} \cdot F_z, \tag{4}$$

$$\mu_y = 1.80 + (-2.14) \cdot 10^{-4} \cdot F_z, \tag{5}$$

where F_z represents the normal force acting on the tire (in N). Once the tire friction coefficients were defined, the limits on the lateral force that could be generated by the tires could be determined.

C. Lateral force limit of the tires

The cornering velocity of a race car is fully defined by the maximum lateral force the tires can handle before losing grip. Therefore, tire friction coefficients are used to determine the maximum velocity as a function of the radius. This is done by limiting the centrifugal force, F_y (in N), to the maximum allowable lateral force on the tires, $F_{y,max}$. The result of this step is shown in Figure 6. Assuming steady state cornering, we can write:

$$F_y = \frac{m \cdot v^2}{abs(R)}, \tag{6}$$

where m (in kg) is the mass of the race car and v (in m/s) is the velocity. Limiting F_y to the maximum lateral friction gives:

$$F_{y,max} = F_{y,f} + F_{y,r} = F_y, \tag{7}$$

where $F_{y,f}$ and $F_{y,r}$ (in N) are the maximum front and rear lateral forces (distributed equally over the two front/rear tires), given by:

$$F_{y,f} = \mu_{y,f}(F_{z,f}) \cdot F_{z,f}, \tag{8}$$

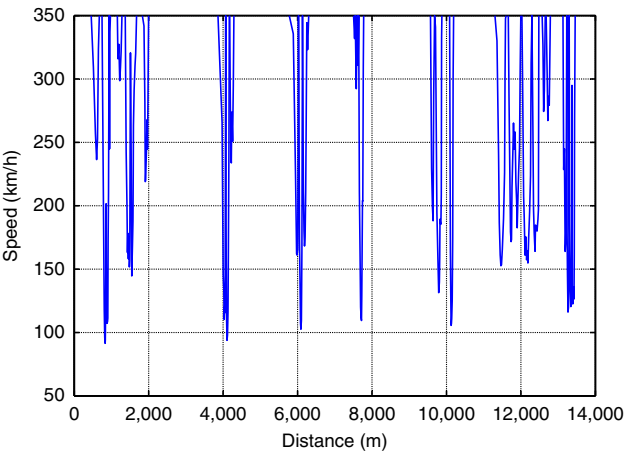

Figure 6.
Maximum velocity due to the lateral tire limit

$$F_{y,r} = \mu_{y,r}(F_{z,r}) \cdot F_{z,r}. \tag{9}$$

Assuming a linear fit to the tire data, $\mu_{y,f}$ and $\mu_{y,r}$, the tires' lateral friction coefficients, can be expressed as:

$$\mu_{y,f} = c_3 + \frac{c_4}{2} \cdot F_{z,f}, \tag{10}$$

$$\mu_{y,r} = c_3 + \frac{c_4}{2} \cdot F_{z,r}. \tag{11}$$

Here the coefficient C_4 is divided by two, to account for the fact that the tire data is for a single tire. For the normal forces $F_{z,f}$ and $F_{z,r}$ we can then write:

$$F_{z,f} = \frac{(m \cdot g + F_{down}(v)) \cdot L_r}{L}, \tag{12}$$

$$F_{z,r} = \frac{(m \cdot g + F_{down}(v)) \cdot L_f}{L}, \tag{13}$$

where m is the mass of the race car (in kg), L is the length of the race car (in m), and L_f and L_r are the lengths from the center of gravity to the front and rear axle (in m), respectively. F_{down} is the downforce of the race car (in N) and is dependent on the speed according to:

$$F_{down} = \frac{1}{2} C_{dd} \cdot \rho_{air} \cdot A_f \cdot c_d \cdot v^2, \tag{14}$$

with C_{dd} being the drag-to-downforce ratio, ρ_{air} the air density (in kg/m^3), A_f the frontal area of the race car (in m^2), and c_d the drag coefficient. The drag coefficient is a measure of the drag-force created by the car's body, while the drag-to-downforce ratio is a relation between the drag force and the downforce generated by the car's body. A higher value of c_d could mean a lower straight line acceleration, however, when combined with a higher value of C_{dd}, this can lead to higher cornering speeds.

After considering the limits on speed imposed by the lateral force generated by the tires, the next step was to account for the limits imposed on the achievable speed by the available braking force.

D. Brake limit

Any race car has limited braking capabilities, which limits the allowable velocity at a time instant that precedes braking. Having the velocities given by lateral tire limits at each GPS position, the track is scrutinized in a backwards fashion. First, the final GPS position is analyzed, after which the previous GPS position is analyzed, and so on. At every point, it is checked whether the velocity is limited by the brakes or lateral force limit of the tires. This is represented by:

$$v_{max} = min(v_{braking}, v_{lat}). \tag{15}$$

This limit then becomes the new maximum velocity and the new initial velocity for the next point. The result is shown in Figure 7. The maximum deceleration, a_{min} (in m/s^2), is dependent on the longitudinal component of the gravitational force, F_g (in N), the friction force, F_f (in N), the drag force, F_d (in N), and the brake force, F_b (in N) as:

$$a_{min} = -\frac{F_g + F_f + F_d + F_b}{m}. \tag{16}$$

Here, the longitudinal gravitational force as a function of the gradient θ (in rad) is given by:

$$F_{g,x} = m \cdot g \cdot \sin(\theta), \tag{17}$$

the friction force is expressed as:

$$F_f = c_d \cdot \cos(\theta) \cdot (m \cdot g + F_{down}), \tag{18}$$

the drag force can be written as:

$$F_d = \frac{1}{2} \cdot \rho_{air} \cdot A_f \cdot c_d \cdot v^2, \tag{19}$$

and the brake force is written as:

$$F_b = F_{x,f} + F_{x,r}, \tag{20}$$

where $F_{x,f}$ and $F_{x,r}$ are the front and rear longitudinal forces (in N) given by:

$$F_{x,f} = \mu_{x,f}(F_{z,f}) \cdot F_{z,f} \tag{21}$$

$$F_{x,r} = \mu_{x,r}(F_{z,r}) \cdot F_{z,r}. \tag{22}$$

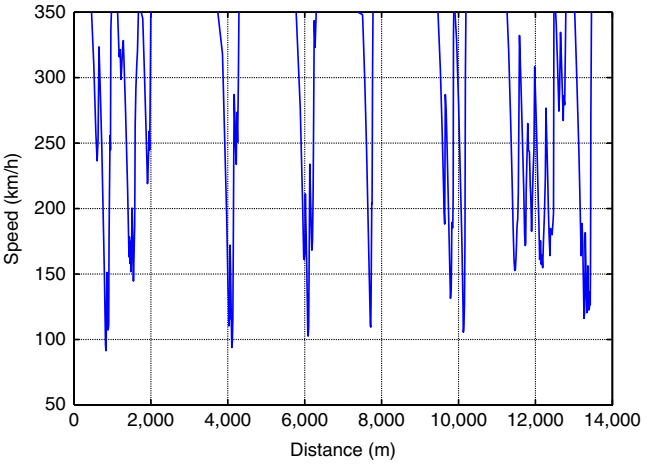

Figure 7.
Maximum velocity due to the lateral tire limit and brake limit

Assuming a linear fit to the tire data, $\mu_{x,f}$ and $\mu_{x,r}$, being the tires' longitudinal friction coefficients, can be expressed similar to Equation (10) as:

$$\mu_{x,f} = c_1 + \frac{c_2}{2} \cdot F_{z,f}, \tag{23}$$

$$\mu_{x,r} = c_1 + \frac{c_2}{2} \cdot F_{z,r}. \tag{24}$$

The normal forces $F_{z,f}$ and $F_{z,r}$ can be written as:

$$F_{z,f} = F_{z,total} - F_{z,r} = F_{g,z} + F_{down} - F_{z,r}, \tag{25}$$

$$F_{z,r} = \frac{-B + \sqrt{B^2 - 4 \cdot A \cdot C}}{2 \cdot C}, \tag{26}$$

with:

$$A = -F_{z,total} \cdot (L_f + c_1 \cdot h_{cog}) + 2h_{cog}(F_{g,z}^2 + 2F_{g,z} \cdot F_{down} + F_{down}^2), \tag{27}$$

$$B = L - 2 \cdot c_2 \cdot h_{cog} \cdot F_{z,total}, \tag{28}$$

$$C = 2 \cdot c_2 \cdot h_{cog}, \tag{29}$$

and the gravitational force in direction perpendicular to the surface, $F_{g,z}$ (in N) given by:

$$F_{g,z} = mg \cdot \cos(\theta). \tag{30}$$

Once the limits imposed by the available braking force were taken into account, the next step was to consider the achievable acceleration.

E. Acceleration limit

The acceleration limit is mainly due to power and traction limitations and can be expressed as:

$$\min((F_m - F_d - F_{g,x} - F_f), F_{x,max}), \tag{31}$$

where F_m is the force the motor can apply on the tires (in N), and $F_{x,max}$ is the maximum force the tires can handle (in N). F_m is written as:

$$F_m = \frac{2 \cdot T \cdot M \cdot T_g}{D_{tire}}, \tag{32}$$

with T being the available torque at the current speed (in Nm), M the number of motors, T_g the gear ratio, and D_{tire} the tire diameter (in m). $F_{x,max}$ is written as:

$$F_{x,max} = F_{x,f} + F_{x,r}. \tag{33}$$

See Equations (21) to (30) for $F_{x,f}$ and $F_{x,y}$.

The drive cycle as calculated using the described method is shown in Figure 8. As a comparison, the speed profile of the Le Mans Audi R18 e-tron quattro is added. Apparently, the largest time gain is at higher acceleration and higher top speed. The corner speed is usually very similar. This is most likely due to the high vehicle mass and Formula 3 tire data. The corners where the speed of the InMotion race car is much higher can be because of a low-grip surface on the real race track or driver limitation. Also corner dynamics (i.e. load transfers) are not taken into account, which would change the real cornering speed.

After the process of deriving the drive cycle was set up, the most feasible technologies for the powertrain components were selected based on the requirements of InMotion. Following this, a preliminary electrical analysis was performed on the powertrain.

IV. Preliminary electrical analysis of the powertrain

Once the technologies for the various powertrain components was selected, it was also essential to analyze the impact of the functioning of various electrical powertrain components on one another. Hence a preliminary electrical analysis of the powertrain was performed. For this analysis, a powertrain with eight motors, eight generators, four DC-DC converters, eight DC-AC converters, a set of ultracapacitors, and four sets of DC-link capacitors was considered. Figure 9 displays part of this electrical scheme, including the values of the voltages. The working voltage of the motors is 700 V, of the DC-DC converter 200-530 V. The upper limit on ultracapacitor operating voltage is determined by the state-of-charge, which should not be for safety reasons above 80 percent. The lower limit on voltage is determined by the value of DC-DC converter working voltage with a small safety margin. Thus the voltage operating range of the ultracapacitors is 213.8 and 427.6 V.

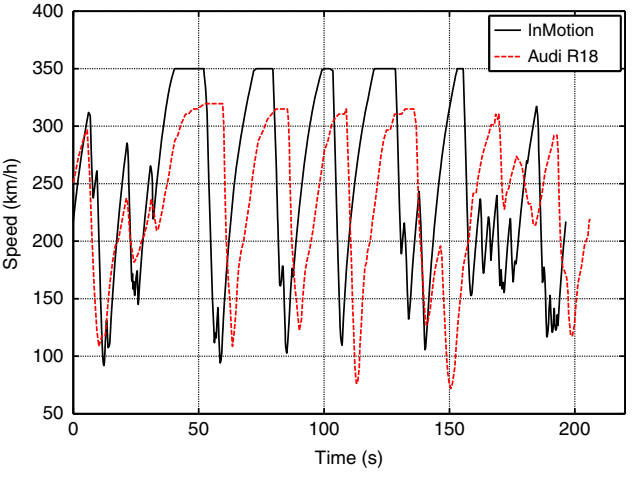

Figure 8.
Drive cycles on Circuit de la Sarthe for InMotion and the Audi R18 e-tron quattro

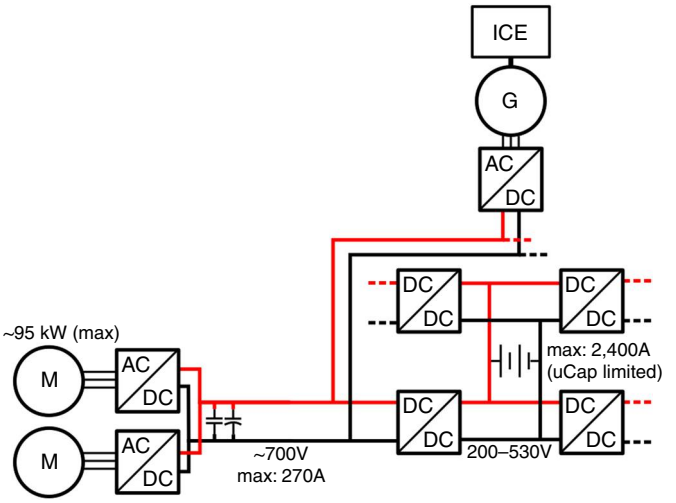

Figure 9.
Part of the electrical scheme of the powertrain architecture

The energy flow in the system is bi-directional, thus motors operate in both motoring and generating mode. During the motoring mode, energy is supplied from the DC-link to the motors. If the energy request is higher than the energy that can be delivered, the voltage on the DC-link will drop significantly, limiting the power produced by the motors. During the generating mode, the energy should be stored fast enough to avoid a rapid rise in voltage on the DC-link, which would damage the components.

The motors are capable of a more dynamic operation when compared the DC-DC converters and the ICE coupled with the generator. This difference in dynamics could cause the DC link to fail. To make sure that the DC-link can still handle these dynamics, sets of capacitors installed at close proximity to the motors has to be added. These sets should consist of both electrolytic and ceramic capacitors. The former is to add capacity; the latter is to handle the power.

To calculate the exact amount of DC-link capacitors needed, a full analysis of the dynamics of the system should be performed. This full analysis of the dynamics was not part of this research and is recommended for future research.

Once the preliminary electrical analysis was performed, a preliminary investigation into the sizings of the various powertrain components was performed to minimize the laptime. This is described in the next section.

V. Lap time sensitivity analysis

A key requirement from the powertrain was to achieve a lap time of 2 min 45 s. Increased sizes of the powertrain components meant an increase in mass of the race car, thus sometimes reducing the performance. Aerodynamic characteristics also had a significant impact on the performance of the vehicle. Hence a sensitivity analysis was performed in order to gain insight into the impact of component sizings and aerodynamic characteristics on the laptime of the vehicle. Three parameters were considered for the sensitivity analysis. The first parameter was the number of motors n_m, since this determined the sizes of the other powertrain components and hence the vehicle mass. The second and third parameters were the drag coefficient c_d and the drag-to-downforce ratio C_{dd}, since these are the key aerodynamic characteristics

of the race car. The number of motors n_m was varied as 4, 6, 8, or 10. The drag coefficient c_d was varied as 0.3, 0.4, 0.5, 0.6, or 0.7 and the drag-to-downforce ratio C_{dd} was varied as 3, 6, 9, or 12. A higher drag coefficient c_d will cause higher drag force and smaller acceleration. However, a high drag coefficient c_d and a high drag-to-downforce ratio C_{dd} result in a higher down force and this increases the maximum speed at the corner. Thus, in total, $4 \times 5 \times 4 = 80$ sets (combinations) of parameters were obtained. The mass of the powertrain components is presented in Table II.

An average efficiency of 85 percent for motor and generator is incorporated in the drive cycle. This helps in accounting for the fact that more generators would be needed than motors, so as to compensate for losses. At the same time, this also helped in sizing the engine to approximately account for generator and motor losses. In addition, the engine is assumed to run at $\vartheta_{ice} = 90$ percent of the maximum power. The reason is to have a safety margin when doing the matching with the backwards model, Section VI. Required number of generators and the ICE power are calculated with these equations:

$$n_g = \frac{n_m}{\eta_m} \tag{34}$$

$$P_{ice} = \frac{P_m \cdot n_m}{\vartheta_{ice} \cdot \eta_m^2} \tag{35}$$

where n_m is number of motors and η_m is motor efficiency. Table III presents the number of generators, total mass of the car and ICE power and mass for different number of motors.

The drive cycle presented in Section III determines the lap time for 80 different sets of parameters shown in Figure 10. Each subplot shows the result for one drag-to-downforce ratio. It can be seen that the lap time decreases with increasing C_{dd}. When the value of drag-to-downforce ratio C_{dd} is 3, more motors results in decrease of lap time. However, for higher values of C_{dd}, there are no significant differences between lap time for eight motors and for ten motors. For four motors, the

Table II. Masses of different components

Components	Masses
DC/DC converter	33 kg×4
Ultracapacitors	200 kg
Chassis	400 kg
Motor	23 kg
Generator	23 kg
ICE	1 kg/2.6 kW

Table III. Number of generators, ICE power and mass, and total mass of the car for different number of motors

n_m	n_g	P_{ice} (kW)	m_{ice} (kg)	Car mass (kg)
4	5	548.1	211	1,247
6	8	822.15	316	1,473
8	10	1,096.2	422	1,677
10	12	1,370.2	527	1,880

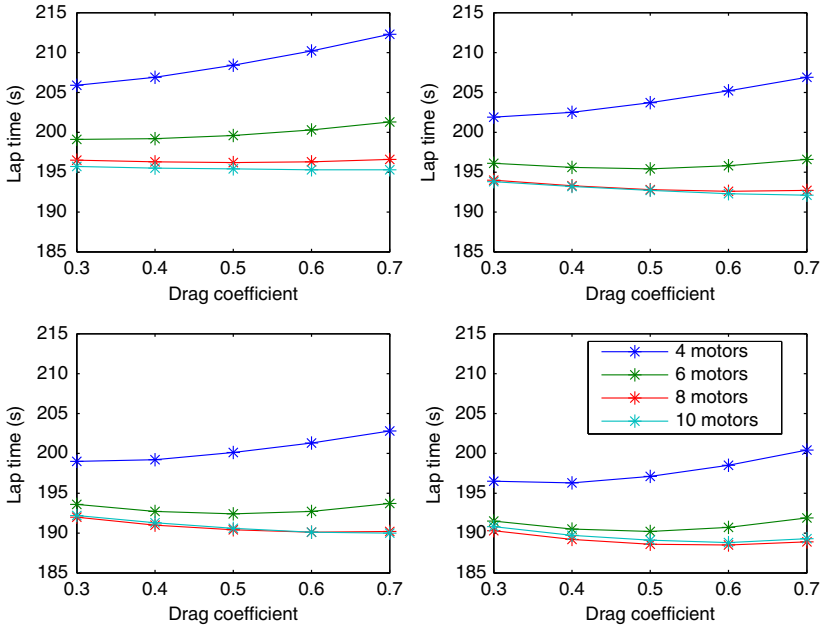

Figure 10.
From left to right and top to down: lap time for drag-to-downforce ratio of 3, 6, 9, 12

lap time increases when c_d increases, that means the drag force at straights has more impact than the down force at the corners. For six motors, the lap time is the lowest when $c_d = 0.5$. For eight and ten motors, the lap time tends to decrease when c_d increases. It was found that using eight motors with a drag-to-downforce ratio of 12 and a drag coefficient of 0.6, yielded the lowest possible lap time. However, using eight motors, would require ten generators and a relatively large engine, which would result in a heavy powertrain and a higher fuel consumption. Although InMotion had not specified any constraints on fuel consumption, the authors decided to include multiple sets of powertrain sizings, in order to clearly demonstrate the penalty on race car mass and fuel consumption as the lap time was decreased. Finally, four feasible sets of parameters were chosen and are shown in Table IV. The sets were selected because they yielded the lowest lap times among all possible combinations of parameters. Three sets have drag ratio C_{dd} of 9 and one set has C_{dd} of 12.

To decrease the lap time, active aerodynamics was modeled by increasing the drag coefficient at the straights and decreasing it at the corners. This enhances both the acceleration limit and the limit on the lateral force that can be generated by the tire. A new analysis with active aerodynamics was done for four chosen sets, in which drag

Set no.	n_m	C_{dd}	Lap time (constant c_d)	Lap time (active $*c_d$)
1	4	9	199.0 – 0.3	193.2 – 0.3-0.7
2	6	9	192.4 – 0.5	189.2 – 0.3-0.7
3	8	9	190.1 – 0.6	188.5 – 0.3-0.7
4	8	12	188.5 – 0.6	186.7 – 0.3-0.7

Note: $*c_d$ is 0.3 at straights and 0.7 at corners

Table IV.
Four sets of parameters

coefficient c_d is 0.7 at the corners and 0.3 at the straights. Table IV presents these four sets and the lap times with fixed and varied c_d. It can be seen that in all cases, active aerodynamics results in a reduction in lap time. Additional insight can be obtained by analyzing the acceleration profiles, as shown in Figure 11. It can be concluded that only the car with ten motors has a comparable profile to the Formula 1 car. Simulations showed that the cars with four, six, and eight motors can have a Formula 1 – comparable acceleration profile if the mass of the car can be reduced 600, 400, and 200 kg, respectively. It can be seen from Table IV that the lowest lap time (188.5 s), with the available technologies, is still 23.5 s above the requirement of being faster than 2 min 45 s (165 s). The acceleration profile of the model is worse than the acceleration profile of the Formula 1 car (2004 season). To decrease the lap time, the components masses should be reduced. Furthermore, the lap time may be reduced by the tires with higher friction capability than that of the Formula 3 tires used in the model.

Once the feasible powertrain component sizes have been defined, the race car had to modeled. To optimize the flow of energy through the powertrain, two Energy Management Strategies (EMS) were developed. One was the boost strategy, based on the hypothesis that fuel can be saved by assisting the engine on the track regions where it needs to accelerate the vehicle right after the braking regions. This strategy is similar to the KERS used currently in Formula 1 vehicles (Formula 1,), with the difference that the energy is delivered completely after the regenerative braking mode. The other energy management strategy was the Equivalent Consumption Minimization Strategy (ECMS), based on optimal control theory (Hofman, 2007). The modeling of the race car, as well as the design and implementation of the EMS on the feasible sets of powertrain sizes are described in the next section.

VI. Modeling and optimization

There are two major approaches to modeling vehicles: the forwards modeling approach and the backwards modeling approach. In the forward modeling approach, the vehicle model incorporates the physical characteristics of the various powertrain components. This approach accounts for the physical causality of the powertrain components, but increases the required computation time. The powertrain of the

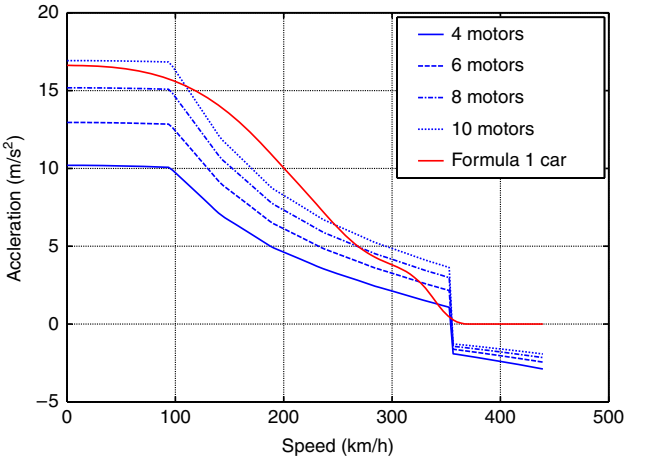

Figure 11.
Acceleration profiles of the cars with four, six, eight, ten motors and the Formula 1 car

InMotion race vehicle was modeled using the backwards modeling approach. The main advantages of using this approach are:

- suitability for the design of supervisory control systems that optimize the power flow in the propulsion system;
- reduction of computation time;
- simplification of modeling of efficiency conversion between powertrain components; and
- reasonable accuracy of fuel consumption calculations (Guzzella and Sciarretta, 2007).

The main drawback of using the backwards modeling approach is that the physical causality is not respected and therefore, dynamic effects are not properly addressed. However, this does not significantly impact the accuracy of the fuel consumption calculations (Guzzella and Sciarretta, 2007). The input variables come from the driving cycle calculation, which is explained in Section III. The force F_t acting on the wheels was computed taking into account the speed and acceleration required to drive the predefined drive cycle. After that, the power flow was estimated for the different powertrain components and finally, the fuel consumption to drive the predefined drive cycle was predicted. More information about the backwards modeling approach can be found in Guzzella and Sciarretta (2007).

The powertrain was modeled using the backwards approach with the following assumptions:

- the driving cycle (speed profile) is known in advance;
- the vehicle runs at a constant speed and acceleration for a short period of time i, which was considered to be 0.1 s;
- the fuel tank mass is constant during the simulation; and
- the transient response of the powertrain components is not included.

In this study, the backwards modeling approach was used to optimize the energy flow of the powertrain using different supervisory control strategies. Moreover, the backwards model helped in finding the trade-off between sizing the components, fuel consumption, and the impact on lap time.

A. Modeling description

Based on the powertrain layout shown in Figure 12, powertrain component input and output requirements were modeled using the backwards modeling approach. Vehicle dynamics were implemented using Newton's second law. The total force acting on the vehicle was calculated based on following equations:

$$F_{t,i} = m \cdot a_i + F_{r,i} + F_{a,i} + F_{g,i}, \tag{36}$$

where:

$$F_{r,i} = m \cdot g \cdot \cos(\alpha_i), \tag{37}$$

$$F_{a,i} = \frac{1}{2} \cdot c_d \cdot \rho_a \cdot A_f \cdot c_d \cdot v^2, \tag{38}$$

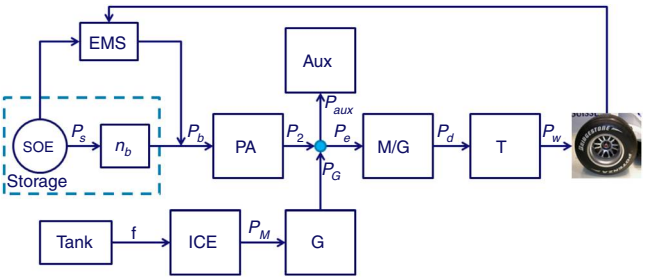

Notes: T, Transmission; M/G, motor/generator; Aux, auxiliary power demand; G, generator; ICE, internal combustion engine; PA, DC/DC converter; EMS, energy management strategy; SOE, state of energy

Figure 12.
Series topology

$$F_{g,i} = m \cdot g \cdot \sin(\alpha_i), \tag{39}$$

where $F_{t,i}$ (in N) represents the force acting on the wheels, $F_{r,i}$ (in N) represents the rolling friction, $F_{a,i}$ (in N) the aerodynamic friction, $F_{g,i}$ (in N) the force caused by gravity when the road has an inclination angle α_i (in rad), A_f (in m^2) the frontal area of the vehicle, and ρ_a (in kg/m^3) the density of air. c_d is the drag coefficient, m is the vehicle mass, g is the acceleration due to gravity (in m/s^2), and a_i is the acceleration of the vehicle (in m/s^2).

The power at the wheels required to drive the predefined profile, $P_{w,i}$ (in W), was computed as follows:

$$P_{w,i} = T_{w,i} \cdot \omega_{w,i}, \tag{40}$$

where:

$$T_{w,i} = F_{t,i} \cdot R_w, \tag{41}$$

$$\omega_{w,i} = \frac{v}{R_w}, \tag{42}$$

where $T_{w,i}$ represents the torque acting on the wheels (in Nm), $\omega_{w,i}$ the angular speed of the wheels (in rad/s), v the vehicle speed (in m/s), and R_w the wheel radius (in m). The power at the wheels is calculated by using the balance of forces acting on a vehicle in motion, see (36).

The power at the input of the gearbox $P_{d,i}$ (in W) was modeled with the following equation:

$$P_{d,i} = T_{d,i} \cdot \omega_{gb,i}, \tag{43}$$

with:

$$T_{d,i} = \begin{cases} \frac{T_{w,i}}{\eta_{gb}} \cdot r_g & T_{w,i} \geq 0 \\ T_{w,i} \cdot \eta_{gb} \cdot r_g & T_{w,i} < 0 \end{cases} \tag{44}$$

and:

$$\omega_{gb,i} = \frac{\omega_{w,i}}{r_g}, \tag{45}$$

where r_g represents the gear ratio. The efficiency of the gearbox η_{gb} was assumed to be constant with a value of 0.98. The selection of the fixed gear ratio was done to match the maximum electric motor rotational speed with the maximum wheel speed due to the driving cycle. The value was calculated as $r_g = 0.47$.

The electric motor that was chosen was the Yasa 400. It is a permanent magnet synchronous machine, and the essential parameters have been listed in Table V.

It was modeled by interpolation of the efficiency map shown in Figure 13. The maximum power limit that can be obtained by regeneration was calculated using the power characteristic of the electric motor in the generating mode. The generator in the powertrain was modeled using the same efficiency map as the electric motor (Yasa 400), with the assumption that efficiencies in the generating regime are a mirror image of that in the motoring regime.

Max Peak Power (kW)	165
Peak Torque (Nm)	400
Max RPM	7,500
Rated RPM	3,500
Max Cont. Power (kW)	90
Max Cont. Torque (Nm)	245
Mass (kg)	20
Specific Power (kW/kg)[a]	4.5
Specific Torque (Nm/kg)[b]	12.3

Notes: [a]Calculated with maximum continuous power; [b]calculated with maximum continuous torque

Table V.
YASA 400 motor parameters

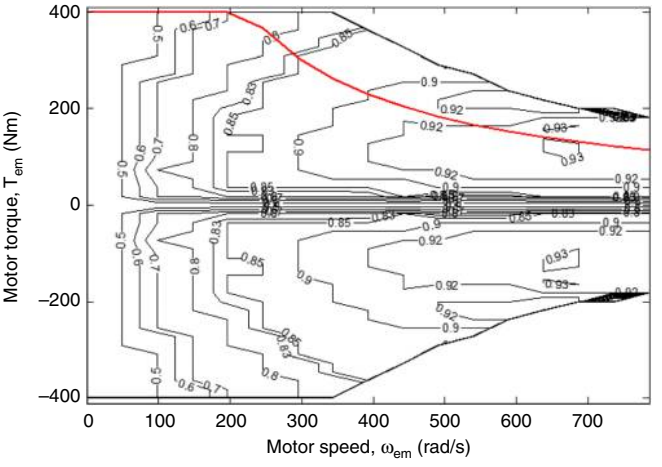

Figure 13.
Yasa 400 motor/ controller efficiency map

The energy storage device (ultracapacitors) was modeled using an efficiency map, using the following equation:

$$P_{2,i} = \begin{cases} P_{b,i} \cdot \eta_{DC} & P_{b,i} \geq 0 \\ P_{b,i} / \eta_{DC} & P_{b,i} < 0 \end{cases} \quad (46)$$

where $P_{2,i}$ represents the output power of the DC/DC converters (in W) and $P_{b,i}$ the output power of the storage device (in W). The DC/DC converters were modeled with a constant efficiency of 0.97 (Koppen, 2007).

The ICE was modeled using a scaled efficiency map of a 1.9 L TDI standard diesel engine (Hofman, 2010) shown in Figure 14. The ICE and the generator were combined in one efficiency map (genset) in the E-line tracking strategy (Kessels *et al.*, 2008).

The power for the electrical auxiliaries, P_{aux}, was assumed to be constant along the drive cycle, with a value of 40 kW.

B. Results

Four different sets of parameters were found in the sensitivity analysis, as mentioned in Section V. Table VI summarizes the results of the backwards model for each of the combinations. It can be seen that there is a trade-off between fuel consumption and lap time. In addition, having more motors decreases the lap time at the cost of increasing the

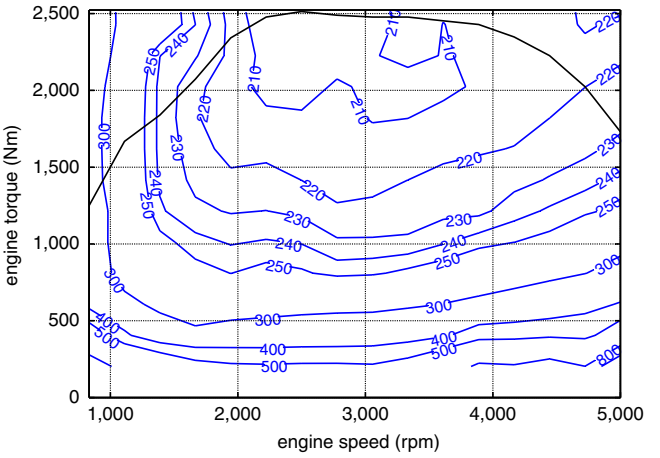

Figure 14.
Engine map (g/kWh)

Set No.	Total mass (kg)	P_{ICE} max (kW)	ICE mass (kg)	FC ECMS (kg/lap)	FC boost (kg/lap)	Lap-time (s)
1	1,242	537	206	3.71	3.95	199.0
2	1,457	780	300	5.04	5.28	192.4
3_a[a]	1,647	1,021	393	6.17	6.38	190.1
3_b[a]	1,652	1,036	398	5.49	5.65	188.7
4	1,634	988	380	6.05	6.29	188.5

Table VI.
Backwards model results for the four sets chosen[a]

Note: [a]Set no. 3_a refers to the simulation using constant c_d and 3_b using varying c_d

size and maximum power required of the ICE, which increases the fuel consumption. Moreover, it can be seen that varying c_d reduces the fuel consumption and lap time, compared to the fixed one. It is worth mentioning that, for simplicity, only one set with varying c_d was simulated with the backwards model (Set No. 3).

For simplicity, only the results for solution 2 (six motors, eight generators, $C_{dd} = 9$, $c_d = 0.6$) are presented in this paper. Figures 15 and 16 show the operating points for the motor and engine, respectively.

The control variable $u = P_s$ (ultracapacitors input power) and the State of Energy (SoE) using the ECMS are shown in Figure 17.

Figure 18 shows the electric power required at the wheels P_e and the input power of the ultracapacitors P_s using the ECMS. Figure 19 shows the same result for a Boost strategy.

To investigate the trade-off between fuel consumption and lap time, the number of theoretical laps that the InMotion vehicle would be able to complete was computed for every of the four sets presented in Table VI. Assuming a fuel density value of 0.83 kg/l (Shell racing fuel,) and a fuel mass of 75 kg per tank, the number of laps that the vehicle

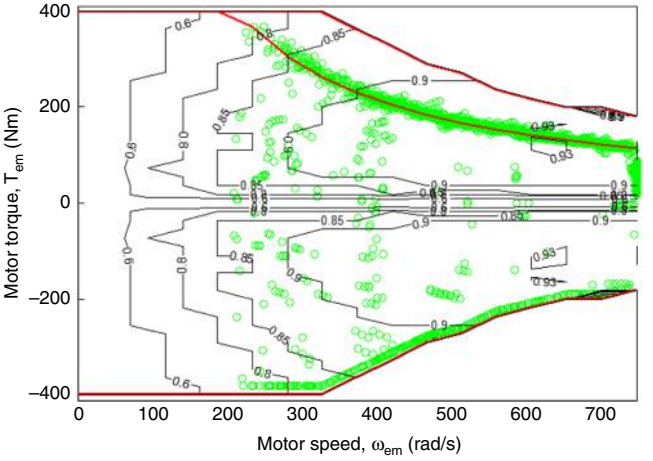

Figure 15.
Motor operating points

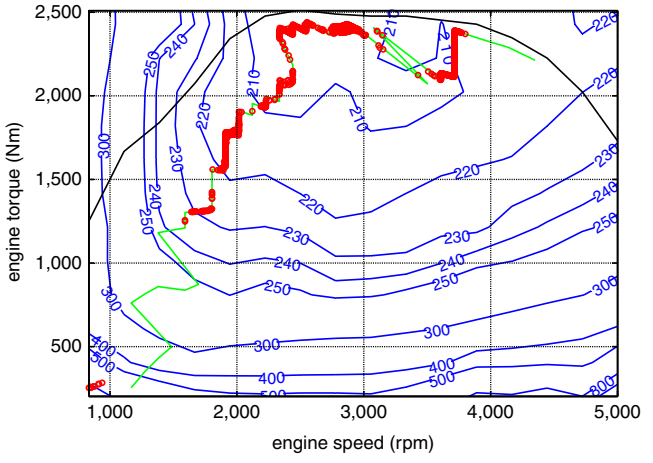

Figure 16.
Engine operating points

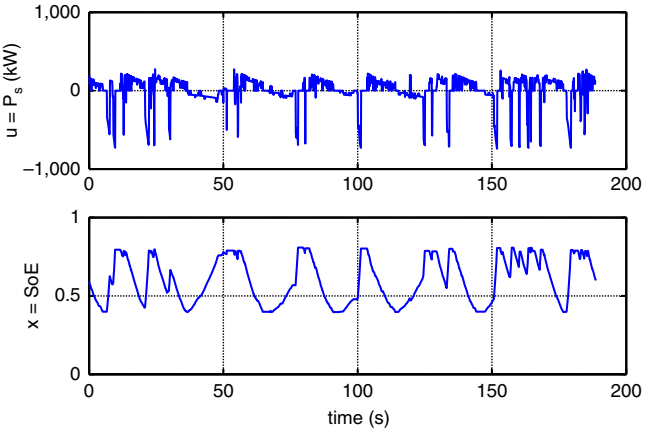

Figure 17.
Ultracapacitors input power using the ECMS

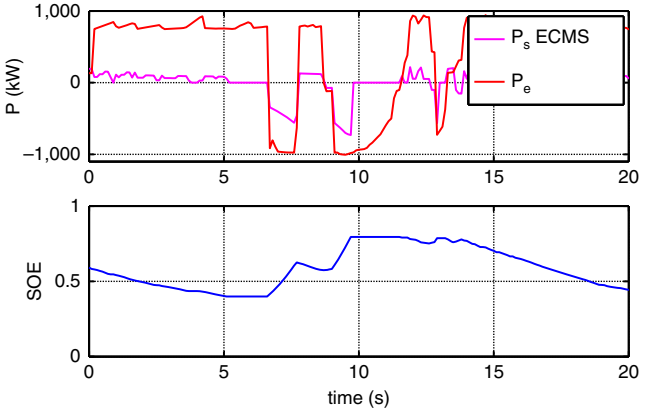

Figure 18.
From top to bottom P_s and P_e using the ECMS, *SoE*

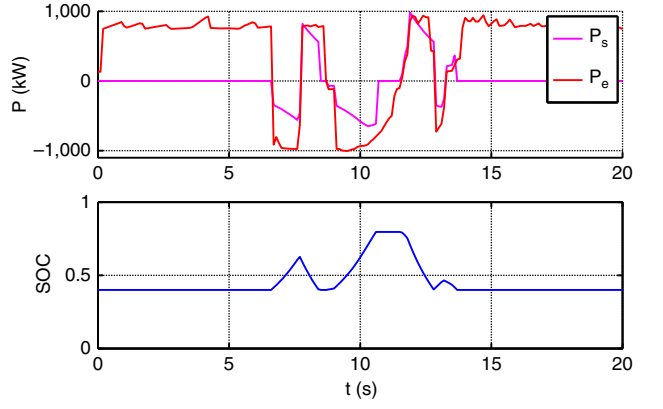

Figure 19.
From top to bottom P_s and P_e using the Boost strategy, *SoE*

could complete was obtained. The total time per pit stop cycle was estimated by, first, computing the number of times the vehicle needs to stop for refueling, and, second, by adding the pit stop time, which in this case was assumed to be 60 s. Table VII presents the results for the completed total number of laps for each of the fours sets for the powertrain, including the one where c_d is varied. It can be seen that there is an improvement of four laps (from 442 to 446 in Set No. 3) when c_d is varied. The number of laps that a Formula 1 car (2004 season) would be able to complete is also shown in Table VII, based on a theoretical lap time of 175 s (see Section II) and a fuel consumption of 75 l/100 km (Formula 1,).

It can be concluded from the results presented above that several options are feasible for designing the powertrain of the InMotion vehicle. The trade-off between fuel consumption and lap time can be better addressed once parameters of more appropriate tires are included in the model, and once more accurate efficiency data for the ICE map is obtained. Moreover, active aerodynamics (varying c_d) and increasing the drag-to-downforce ratio have a positive impact in reducing fuel consumption and lap time, as presented in Tables VI and VII.

VII. Conclusion

This paper presents an initial design of the powertrain for the InMotion IM01 race car. Several powertrain configurations were proposed, where several parameters were varied to investigate their impact on the lap time. A bicycle model was created and used to calculate a drive cycle. In addition, a backwards model was developed, including several efficiency maps, to calculate the overall fuel consumption over the predefined speed profile.

One part of InMotion's vision is to be 10 s faster than a Formula 1 car on Circuit de la Sarthe (i.e. 2 min 45 s, based on the 2008 season). However, with the model created, the fastest lap with one of the proposed configurations (Set No.4, see Table VI) was 3 min 9 s. The large mass was a key factor that prevented the race car with the designed powertrain from achieving the required lap time. In addition, it was found that using more than ten motors would not reduce lap time. However, it is the belief of the authors that using parameters of more appropriate tires in the model will reduce the lap time. Further, using custom-built powertrain components, especially the traction machine, would significantly reduce weight and also contribute to reducing lap time.

All the models and algorithms were made such that they are easily adaptable to any new insights.

The following recommendations are proposed:

- to ensure safe and reliable operation of the electrical components, a full electrical analysis of the powertrain should be performed, as discussed in Section IV;

Set no.	Laps per tank	Total no. of laps	No. of pitstops	Total distance (km)
1	20	428	21	5,833.2
2	15	440	29	5,996.8
3_a[a]	12	443	37	6,037.6
3_b[a]	14	447	32	6,092.2
4	12	446	37	6,078.5
Formula 1[b]	9	476	53	6,487.4

Notes: [a]Set no. 3_a refers to the simulation using constant C_d and 3_b using varying C_d; [b]based on FC = 7.92 kg/lap

Table VII. Theoretical results for the InMotion vehicle in Le Mans

- to further reduce lap time and improve fuel economy, active aerodynamics should be applied;
- to allow higher cornering speeds and higher acceleration/deceleration in the simulation, more suitable tire models should be used;
- to reduce the overall vehicle mass, different possibilities for components integration and reduction of chassis mass should be investigated;
- to enhance the quality of the model, more accurate efficiency maps for the generator, gearbox and ICE should be used; and
- to ensure that the engine power level remains feasible and to reduce the total mass of the vehicle (see Table VI), a powertrain configuration with four motors should be used.

References

Audi. 'Audi R18 e-tron quattro", available at: www.audi.co.uk/audi-innovation/audi-motorsport/audi-r18-etron-quattro.html (accessed 9 2012).

Benson, K.W., Fraser, D.A., Hatridge, S.L., Monaco, C.A., Ring, R.J., Sullivan, C.R. and Taber, P.C. (2005), "The hybridization of a Formula race car", *IEEE Conference Vehicle Power and Propulsion, September*, pp. 295-299.

Formula 1. 'Kinetic energy recovery systems (KERS)", available at: www.formula1.com/inside_f1/understanding_the_sport/8763.html (accessed 9 2012).

Formula 1. 'Inside F1/Engine-gearbox", available at: www.formula1.com/inside_f1/understanding_the_sport/5280.html (accessed 9 2012).

F1 Fanatic. 'How quick would F1 lap at Le Mans", available at: www.f1fanatic.co.uk/2008/06/14/how-quick-would-f1-lap-at-le-mans (accessed 1 2013).

Google. 'Google Earth", available at: www.google.com/earth/index.html (accessed 10 2012).

Guzzella, L. and Sciarretta, A. (2007), *Vehicle Propulsion Systems*, 2nd ed., Springer Ed, Berlin.

Hofman, T. (2007), "Framework for combined control and design optimization of hybrid vehicle propulsion systems", PhD thesis, Eindhoven University of Technology.

Hofman, T. (2010), "Electric and hybrid propulsion systems", lecture notes, Eindhoven University of Technology, Eindhoven.

Hybrid GeoTools. '3D route builder for Google Earth", available at: www.hybridgeotools.com/html/3d_route_builder.html (accessed 10 2012).

Kessels, J.T.B.A, Koot, M.W.T., van den Bosch, P.P.J. and Kok, D.B. (2008), "Online energy management for hybrid electric vehicles", *IEEE Transactions on Vehicular Technology*, Vol. 57 No. 6, pp. 3428-3440.

Koppen, E. (2007), "Control and specification of a (series-hybrid) electric vehicle", internship report, Eindhoven University of Technology, Eindhoven.

Lambert, S., Maggs, S., Faithfull, P. and Vinsome, A. (2008), "Development of a hybrid electric racing car", *Hybrid and Eco-Friendly Vehicle Conference, IET, Coventry*, pp. 1-5.

Paulides, J.J.H., Gysen, B.L.J., Meessen, K.J., Tang, Y. and Lomonova, E. (2011), Influence of multiple air gaps on the performance of electrical machines with (semi) Halbach magnetization", *IEEE Transactions on Magnetics*, Vol. 47 No. 10, pp. 2664-2667.

Shell racing fuel. 'Diesel LM24", available at: http://shellracing.com.au/shell_diesel_LM24_racing_fuel.html (accessed 9 2012).

Sibley, J. and Emadi, A. (2010), "A control analysis of high-performance hybrid electric vehicles", *IEEE Vehicle Power and Propulsion Conference (VPPC), Chicago, IL*, pp. 1-6.

Wolfram Mathworld. 'SSS theorem", available at: http://mathworld.wolfram.com/SSSTheorem.html (accessed 9 2012).

YouTube. 'One lap of the Circuit De La Sarthe with Marcel Fssler in the Audi R18 e-tron Quattro", available at: www.youtube.com/watch?v = DRJHYc3ubxI (accessed 9 2012).

Corresponding author
J. Jacob can be contacted at: jubin.jacob@gmail.com